RESEARCH ARTICLE

CrossMark

New mechanisms of phenytoin in calcium homeostasis: competitive inhibition of CD38 in hippocampal cells

Leila Sadeghi[1] (iD) · Reza Yekta[1] · Gholamreza Dehghan[1]

Abstract

Purpose Phenytoin is a major anticonvulsant drug that is effective to improve arrhythmia and neuropathic pain. According to early works, phenytoin affected cell membrane depolarization by sodium channel blocking, guanylyl and adenylyl cyclase suppression that cause to intracellular Na^+ and Ca^{2+} downregulation. This study was aimed to clarify some ambiguities in pathophysiological action of phenytoin by in vitro and molecular docking analyses.

Methods In this study intracellular free Ca^{2+} of primary culture of embryonic mouse hippocampus evaluated via Fura 2 as fluorescent probe. The effects of phenytoin on ADP ribosyl cyclase activity was assessed by recently developed fluorometric assay. Molecular docking simulation was also implemented to investigate the possible interaction between phenytoin and CD38.

Results Our results confirmed phenytoin competitively inhibits cyclase activity of CD38 ($IC_{50} = 8.1$ μM) and reduces cADPR content. cADPR is a Ca^{2+}-mobilising *second messenger* which binds to L-type calcium channel and ryanodine receptors in cell and ER membrane and increases cytosolic free Ca^{2+}. Ca^{2+} content of cells decreased significantly in the presence of phenytoin in a dose dependent manner ($IC_{50} = 12.74$ μM). Based on molecular docking analysis, phenytoin binds to deeper site of CD38 active site, mainly via hydrophobic interactions and consequently inhibits proper contact of substrate with catalytic residues specially Glu 226, Trp 186, Thr221.

Conclusion Taken together, one of the anticonvulsant mechanisms of phenytoin is Ca^{2+} inhibition from CD38 pathway, therefore could be used in disorders that accompanied by CD38 over production or activation such as heart disease, depression, brain sepsis, airway disease, oxidative stress and inflammation.

Keywords Phenytoin · CD38 · Competitive inhibition · Calcium homeostasis · Sodium blocker · Membrane depolarization

Introduction

Phenytoin (5,5-diphenylimidazolidin- 2,4-dion, PHT) was synthesized in 1908 but its pharmacologic features were not reported until three decades later [1, 2]. PHT is an anticonvulsant and antiarrhythmic medication was approved by United States Food and Drug Administration in 1953 for the prevention of tonic-clonic seizures and partial seizures [3]. There are some ambiguities in molecular mechanism of PHT but previous studies introduced it as a sodium channel blocker [4, 5]. It binds preferentially to the inactive form of the sodium channel and stabilizes it, so reduces the amplitude of sodium-dependent action potentials through enhancing steady state inactivation [6]. Since the fraction of inactive channels is increased by membrane depolarization as well as by repetitive firing, PHT causes voltage-dependent, use-dependent and time-dependent block of sodium-dependent action potentials by binding to the inactive state [7]. It's believed PHT could prevent Ca^{2+} influx through cell membrane by blocking calcium ion channels and also adenylyl cyclase and guanylyl cyclase [8]. Previously reported, PHT suppressed type I calcium channels during depolarization and attenuated sustained repetitive firing [9]. Early works also showed that Ca^{2+} influx produced by depolarizing agents is inhibited by lower concentrations of PHT through regulation of cAMP and cGMP levels in the brain tissue that possibly leads to attenuation of Ca^{2+}

✉ Leila Sadeghi
l.sadeghi@tabrizu.ac.ir; l.sadeghi66@yahoo.com

1 Department of Animal Biology, Faculty of Natural Sciences, University of Tabriz, P.O. Box 5166616471, Tabriz, Iran

regulatory neurotransmitter also [8]. PHT consumption causes osteomalacia, decrease in bone density, in patients due to interruption in calcium absorbance [10]. The mechanism by which PHT inhibits Ca^{2+} conductance remains incompletely understood yet while reported harsh effects of drug on cell membrane depolarization suggest involvement of other Ca^{2+} regulatory pathways. By considering PHT physiological side effects, this study suggests CD38 as one of the possible goals that produces some secondary messengers in cytosolic Ca^{2+} regulation from extracellular and intracellular sources [11].

CD38 is a 45 KDa transmembrane enzyme which converts wide range of substrates such as nicotinamide adenine dinucleotide (NAD), cyclic adenosine diphosphate ribose (cADPR), nicotinamide adenine dinucleotide phosphate (NADP), nicotinic acid adenine dinucleotide phosphate (NAADP) and nicotinic acid (NA) to related products (cADPR, ADPR, ADPRP, NAADP) [12]. Almost all of the products are related to Ca^{2+} homeostasis in the living system specially cADPR that is Ca^{2+} mobilizing second messenger [12, 13]. cADPR is produced by cyclization activity of CD38 and binds to ryanodine receptor and also L-type calcium channel lead to Ca^{2+} release into the cytosol [13]. Hippocampus is one of the important tissues was undergone by disrupted Ca^{2+} homeostasis in different neurological disorders and is the main subject of Ca^{2+} regulation studies [14]. To investigate the possibly role of PHT in CD38 regulation, we measured cyclase activity related to hippocampal cells in the presence of different concentrations of PHT. Intracellular Ca^{2+} $[Ca^{2+}]_i$ of hippocampal cells that treated by PHT was evaluated as a final result of CD38 activity by a fluorescent probe. This study also investigated the possible interactions between PHT-CD38 and its role in the cyclase activity of hippocampal cells by molecular docking simulation.

Material and methods

Chemicals

Fura-2 pentakis (acetoxymethyl) ester, phenytoin (5,5-diphenyl-2,4-imidazolidinedione), NAD and nicotinamide guanine dinucleotide (NGD) sodium salt were purchased from Sigma Aldrich Company (St. Louis, MO, USA). Tetrodotoxin citrate (TTX) was prepared from Merck Millipore Company. All other solvents and chemicals were of the highest grade-commercially available.

Preparation primary cell culture

Mouse hippocampal primary culture was prepared according to previous studies with some modifications [15, 16]. Neonatal mouse brain (embryonic day 19) was isolated; hippocampus tissue was exposed after remove of striatal, thalamic, and midbrain from medial surface of brain [15]. Dissected hippocampus triturated by trypsin and mechanical disruption. Cells were differentiated in neurobasal medium supplemented with B27 and FGF2 during 7 days [17]. Punch cultures were made by removing triturated tissue from the ventral surface of the brain, medial and caudal to the bifurcation of the medial cerebral artery. The punches produced a flattened cylinder of tissue with magnocellular neurosecretory cells near the ventral tip.

Measurement of $[Ca^{2+}]_i$

To monitor the changes in intracellular cytosolic free calcium concentrations ($[Ca^{2+}]i$), isolated and treated neurons were incubated with 5 μM of Fura2-AM (Fura 2 acetoxymethyl ester) for 1 h at 37 °C as described previously [16, 18]. Cells were resuspended in a calcium-free solution (135 mM NaCl, 5.4 mM KCl, 1 mM $MgCl_2$ and 5 mM Hepes, pH 7.4) and after washing with same solution incubated for 10 min to release the dye from the AM forms by intracellular esterase. Calcium measurements were performed at 37 °C in a 2 ml cuvette, under continuous stirring on a Perkin Elmer luminescence spectrometer LS 55. The excitation wavelength was set at 340 and 380 nm and the emission spectra were recorded at 510 nm. Excitation and emission slit width were set at 5 nm. $[Ca^{2+}]_i$ was calculated based on the fluorescence ratio of 340/380 nm as previously defined [18]. In this study NAD^+ (100 μM) was used as Ca^{2+} inducer and TTX (50 nM) as specific sodium blocker [19]. Cells were pretreated with different concentrations of PHT, TTX and NAD^+ 30 min before the procedure for evaluation their effects on intracellular Ca^{2+} content.

ADPR cyclase activity assay

CD38 is a member of the ADPR cyclase family that converts NAD^+ to cADPR, but is also an ADP hydrolase converting active cADPR to inactive ADP-ribose [12]. Detection and separation of two reactions that proceed simultaneously are difficult; therefore we used an assay that monitors cyclization of NGD^+ to cyclic GDP ribose (cGDPR) [20]. cGDPR is a nonhydrolyzable fluorescent surrogate of cADPR that could be quantitated by fluorimetry. Thus, the rate of cGDPR production, in the absence of its breakdown, will more accurately reflect the ADPR activity of CD38 as standard protocol. For the NGD^+ cyclase assay; 0.8 ml of lysate fraction (after centrifugation) was added to 0.2 ml of 0.1 mM nicotinamide guanine dinucleotide in 20 mM Tris, pH 7.0, and the increase of cyclic GDP-ribose fluorescence was measured at 410 nm with excitation at 300 nm. Excitation and emission slits width set on 5 nm. Enzyme assay was done in the presence of different concentrations of PHT to evaluate PHT effects on cyclase activity modulation and different concentration of GDP

to assess kinetic parameters. All enzyme assays were done at room temperature in three biological replicates.

Molecular docking analysis

Molecular docking was carried out to simulate binding process of PHT to CD38 protein using Auto Dock software (version 4.2) [21]. The crystal structure of CD38 (PDB ID: 4TMF) was taken from the Protein Data Bank (https://www.rcsb.org/). Since chains A and B are completely similar and have same structure, the chain A was selected to perform docking investigation precisely. The 3D molecular structure of PHT was obtained from the PubChem website (https://pubchem.ncbi.nlm.nih.gov/compound/phenytoin) (PubChem CID: 1775). The structural conformation of PHT was minimized based on theoretical level of B3LYP with 6–31G basis set by Gaussian 03 programs. The rotation of PHT was defined and rotatable bonds were detected. In addition, polar hydrogen atoms and Kollman charges were added into CD38 as a target. Lamarckian genetic algorithm (LGA) search method was used for docking calculation to find the best binding site of PHT to CD38. All other calculation parameters were default settings. The obtained PHT-CD38 structure was visualized by using Chimera 1.10.1 program and Discovery studio visualizer 3.5 [22].

Statistical analysis

All experiments were performed in triplicate and values were expressed as the mean ± standard deviation (SD). Data was analyzed using one-way ANOVA followed by the post-hoc Duncan multiple range test for analysis of biochemical data using SPSS version 11. Differences were considered significant at $p < 0.05$.

Results

PHT suppressed calcium entry induced by β-NAD

To investigate the effects of PHT on cytosolic Ca^{2+} regulation from CD38 pathway, we measured intracellular free Ca^{2+} of hippocampal cells in the presence of NAD^+ and PHT. Previous studies have reported 100 μM NAD^+ could trigger Ca^{2+} entry to the cytosol [11]. Our results also showed 100 μM NAD^+ elevates intracellular calcium level more than 2.6 times higher than control; therefore NAD^+ was used as Ca^{2+} up-regulator in this study. The raised intracellular calcium due to NAD^+, were partially inhibited by pre-treatment with PHT (1–50 μM). As shown in Fig. 1a, PHT significantly blocked Ca^{2+} influx into the cells in a concentration dependent manner. The most significant inhibition of the $[Ca^{2+}]i$ was obtained by 25 μM concentration of PHT (6.7 folds). Ca^{2+} influx inhibition constant, the concentration of PHT could suppress half of the Ca^{2+} influx, calculated as 8.01 ± 1.02 μM. We assessed sodium conductance role in $[Ca^{2+}]i$ by blocking the sodium channels via TTX (50 nM) according to previous results [19]. TTX is a specific sodium channels blocker that could not reduce Ca^{2+} influx induced by NAD^+ in the presence or absence of PHT in this study (Fig. 1a).

PHT significantly inhibits ADPR cyclase activity in hippocampal cells

ADPR cyclase activity related to CD38 was measured in hippocampal cell lysate by recently developed fluorometric assay based on measuring the synthesis of fluorescent cyclic GDP-ribose from nicotinamide guanine dinucleotide (NGD^+), the NAD^+ surrogate [23]. We found that CD38 enzyme extracted from primary culture of hippocampal cells synthesizes
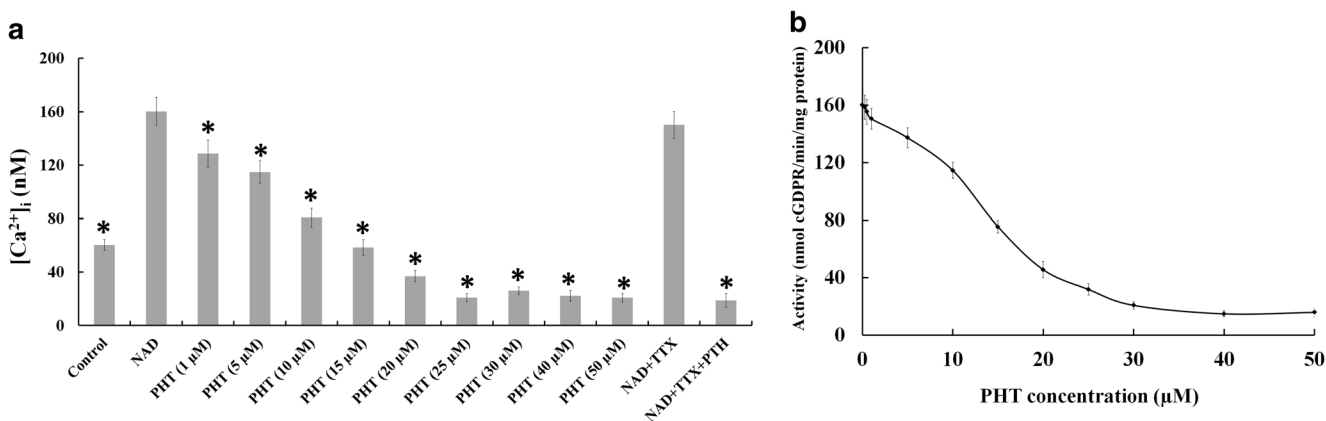

Fig. 1 PHT effects on calcium homeostasis in hippocampal cells. (a) PHT decreased intracellular free Ca^{2+} according to concentration. The data were expressed as mean ± SD of three independent experiments. Asteric (*) symbol indicates significant changes ($p < 0.05$) than $[Ca^{2+}]i$

in the presence of NAD^+ (b) Cyclase activity of CD38 suppressed by different concentrations of PHT. Enzymatic activity decreased to half of maximum in the presence of 8.1 μM inhibitor. The data were expressed as mean ± SD of three independent experiments

cGDPR at a rate of 160.25 ± 9.13 nmol/min/mg protein. As previous study enzyme activity was inhibited significantly by addition of NAD$^+$ due to competition with substrate, therefor we don't use NAD$^+$ in assay medium [23]. PHT inhibited cGDPR formation significantly (Fig. 1b), that related to ADPR cyclase activity of CD38. Maximum inhibition was obtained by 40 μM PHT that reduces enzyme activity to 14.82 ± 2.78 nmol/min/mg protein. The IC$_{50}$ value, concentration of inhibitor that inhibits 50% of the enzyme activity, was estimated to be 12.74 ± 1.47 μM of PHT.

Kinetic parameters of cyclase activity calculated from Michaelis-Menten plot in the presence or absence of PHT (Fig. 2). In order to identify the inhibition mechanism of PHT on CD38, changes in cyclase activity were investigated at room temperature using NGD$^+$ as a substrate in the presence of different concentrations of PHT (0, 5 and 10 μM) and summarized in Table 1. All of the enzyme assays were done at three independent replicates and data expressed as mean ± SD. Results showed the maximum velocity (V$_{max}$) of the enzyme does not change significantly in the presence of 5 or 10 μM of PHT as well as the control (absence of PHT). Apparent K$_m$ that refers to the concentration of substrate which permits the enzyme to achieve half of V$_{max}$ was increased in the presence of PHT.

According to our results (Lineweaver-Burk plot) PHT competes with the substrate, it is intuitively comprehensible that,

at "infinitely" high substrate concentrations, the presence of the inhibitor does not affect the maximal rate of the reaction but decrease the affinity of enzyme to the substrate that interpreted to competitive type of inhibition (Fig. 2). K$_m$ value was enhanced about 1.83 and 2.80 folds in the presence of 5 μM and 10 μM of PHT, respectively which refer to decreased affinity to the substrate. Inhibition coefficient "α" calculated from Lineweaver-Burk plot, slop = αK$_m$/V$_{max}$, interpreted to ratio of K$_m$ in the presence of inhibitor to K$_m$, related to uninhibited reaction. In the assay medium without PHT the value of α is $\approx$1 as expected but α exceeds unit and reaches to 1.83 ± 0.03 and 2.8 ± 0.06 in the assay medium with 5 and 10 μM PHT, respectively. K$_i$ or inhibition constant could be calculated from secondary plot: $\alpha = 1 + [I]/K_i$. Therefore inhibition constant of PHT calculated as K$_i = 5.78 \pm 0.5$ μM.

Molecular docking studies confirmed PHT binding to the CD38 active site

The crystal structures of CD38 in complex with a series of substrates and substrate analogues have provided detailed understanding of the catalytic mechanism of cyclization and hydrolysis by CD38 [24, 25]. To predict the best binding sites of PHT molecule on CD38, molecular docking study was performed by Autodck 4.2. The best binding site of PHT on
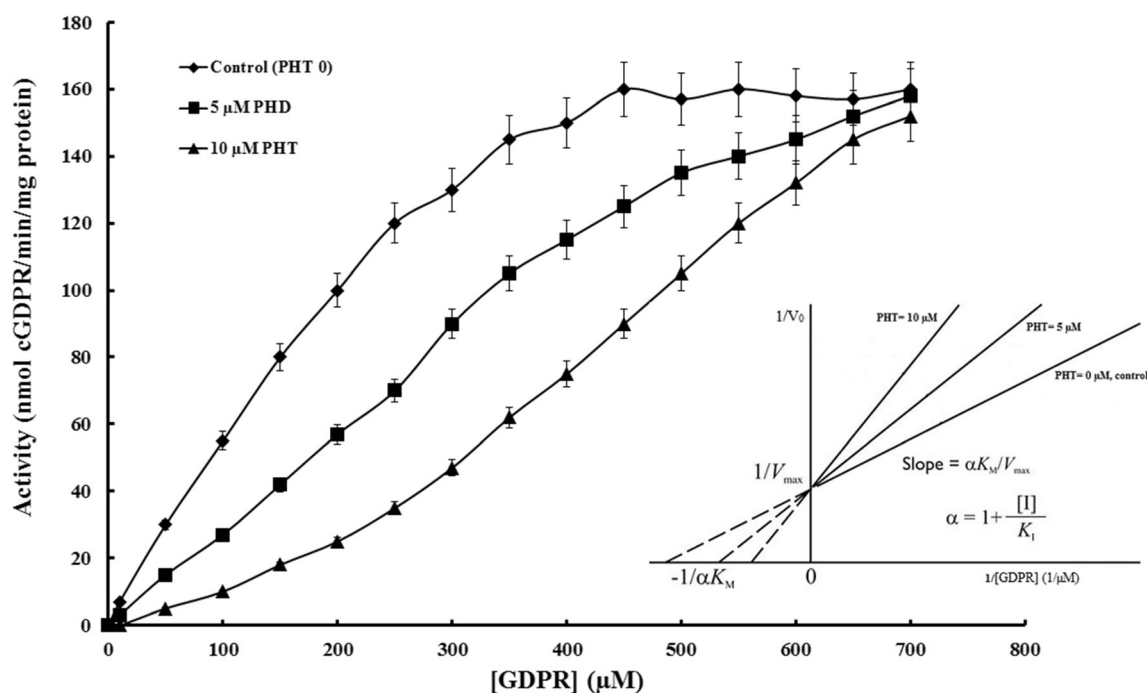

Fig. 2 Cyclase activity related to CD38 that extracted from hippocampal cells in a range of substrate (0–800 μM) resulted to Michaelis-Menten plot in the presence of three different concentration of PHT (0, 5 and 10 μM). CD38 activity decreased in the presence of PHT in a concentration dependent manner. Lineweaver-Burk plot showing the effect of changing inhibitor concentration on 1/-Km (x-intercept) of CD38 conversion of NGD+ to cGDPR. PHT increases K$_m$ without changing V$_{max}$ value in the reaction, consistent with competitive enzyme inhibition. Whole experiment is repeated independently at least three times and results showed mean ± SD

Table 1 Catalytic parameters of cyclase activity in the presence of 5 and 10 μM of PHT in comparison with control (without PHT)

Kinetic parameters	PHT = 0 μM	PHT = 5 μM	PHT = 10 μM
V_{max} (nmol cGDPR/min/mg protein)	160.13 ± 10.48	155.82 ± 11.27	153.45 ± 10.93
K_m (μM)	150.95 ± 9.24	275.17 ± 13.72	420.35 ± 23.82
α (inhibition efficiency)	1	1.83 ± 0.03	2.8 ± 0.06

CD38 is a cavity in the active site; between two α-helixes and β-strand domains (Fig. 3). The docking studies revealed that both of NAD$^+$ and PHT bind to the same catalytic cavity with approximately same binding energies (Fig. 4). Binding energy was calculated as −7.48 kcal/mol for PHT and −7.76 kcal/mol for NAD$^+$. As previously reported the following residues; Trp 189, Glu 146, Asp 155, Tyr 221, Ser 126, Arg 127, Phe 222, Trp 176, Trp 125, Ser 193, Leu 157 and Glu 226 are involved in the interaction between NAD$^+$ and CD38 as the main amino acids in the catalytic activity [25, 28, 29]. The presence of hydrophobic amino acids (Trp 189, Tyr 221, Phe 222, Trp 176 and Trp 125) in CD38 active site produces a hydrophobic environment to PHT binding through hydrophobic rings (Fig. 4). It seems that the main type of interaction in PHT binding is hydrophobic and anion-π interactions. As previously approved, hydrophobic interactions with Trp 189 and Trp 125 participate in the substrate binding [28, 29]. Docking results revealed that the aromatic rings of PHT are closely located to the aromatic rings of amino acids such as Trp 125, Trp 185 (about 3 Å distance); consequently, allows to the π-π interaction. Therefore, it would interrupt the substrate binding to the active site's residues, and following that the catalytic function of CD38 would be inhibited (Fig. 4c) [26, 27]. These results could confirm the results of kinetic study for competitive inhibition. PHT is also close to the Glu 146 that participates in the substrate binding; PHT could interact with the side chain of Glu 146 by anion-π interaction. As Fig. 4d, PHT was interacted with the main catalytic residue Glu 226 by anion-π interaction [25] that could not bind to the substrate in the presence of PHT due to steric repulsion.

Discussion

CD38 is a multifunctional enzyme/receptor was originally identified as a surface antigen on T cells but has since been found in almost all cell types [12, 24, 25]. It consists of an N-terminal cytoplasmic tail, a transmembrane helix and a C-terminal domain with multiple enzymatic activities, catalyzing both cyclization and hydrolysis activities toward different substrates [28]. This enzyme uses several types of mechanisms for different catalytic activities that are done by same active site. NAADP is synthesized during a base-exchange reaction using NADP and NA as substrate [12, 28]. CD38 produces cADPR through a base-exchange, cyclization, and hydrolytic reaction pathways [29]. It can also hydrolyze both NAD$^+$ and cADPR to ADP-ribose [12]. Approximately all of the products are related to Ca^{2+} mobility from different pathways specially cADPR that induced Ca^{2+} release to cytosol from ER and extracellular [24, 25]. By considering Ca^{2+} homeostasis role in membrane depolarization, differentiation and cell death, CD38 hyperactivation plays important role in different diseases such as depression, arrhythmia, brain sepsis, diabetes, AIDS and chronic lymphocytic leukemia [30–33] . Therefore there is a great interest to develop specific and generally applicable inhibitors of CD38 and some inhibitors have been reported recently such as 2,2′-dihydroxyazobenzene and cyclic inosine 59-diphosphate ribose to control of Ca^{2+} influx through CD38 pathway [34, 35]. PHT is an anti-seizure drug could regulate Ca^{2+} current by inhibition of the adenylyl cyclase, guanylyl cyclase, Na$^+$ influx [7, 8] and possibly CD38 pathway that investigated here. This study evaluated cyclase
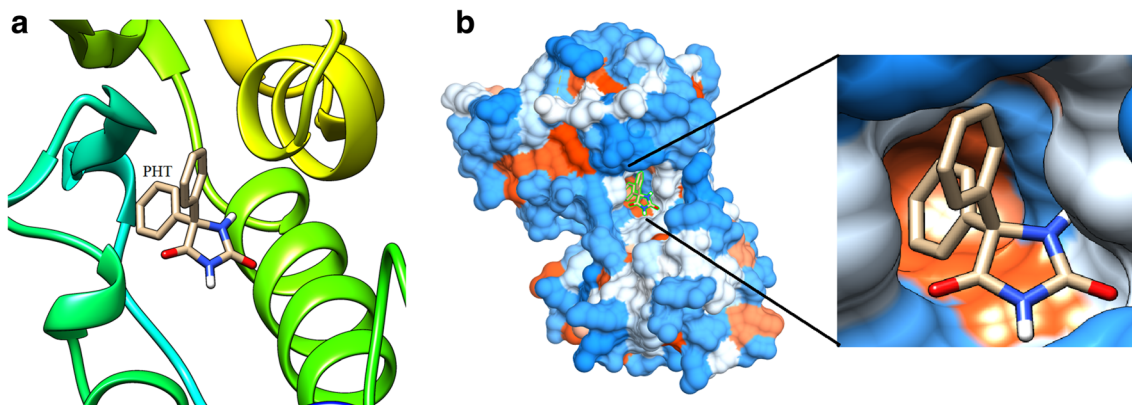

Fig. 3 PHT molecule in the CD38 active site. **a** Interaction of PHT with helix and ribbon related to catalytic site of CD38. **b** Surface view of the active site cavity of the crystal structure of CD38 with PHT bound inside in two resolutions

Fig. 4 PHT and NAD$^+$ located in the CD38 active site. **a** Hydrophobic surface model showed PHT placed in dipper site of catalytic cavity rather than NAD$^+$ that was suppressed to proper placement in active site. PHT was showed by pink color and NAD was visualized as a purple molecule in CD38 active site **b** The carton form of one subunit of CD38 shows substrate binding residues interact with PHT (pink molecule). **c** PHT is located close to the main residues (Glu 226, Glu 146, Asp 155, Trp 189 and Thr125) in the active site of CD38 that have important roles in the substrate binding and catalytic activity. **d** Different interactions between PHT and the active site's residues, especially Glu 226 as a main catalytic residue
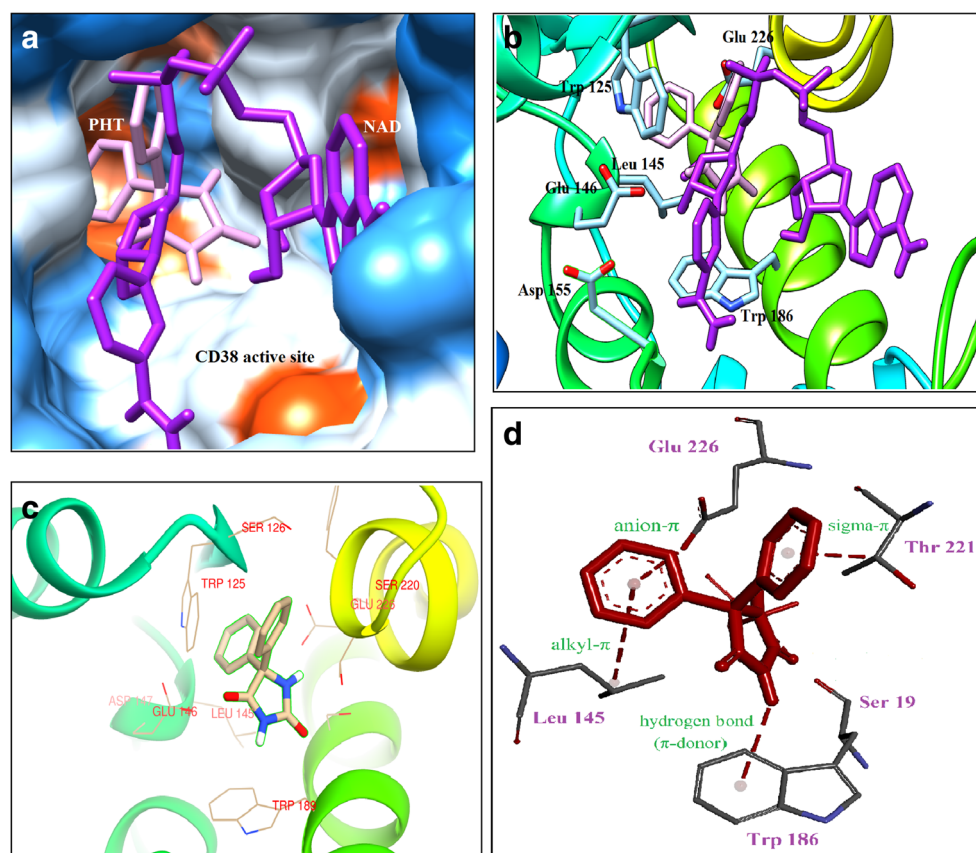
activity of CD38 extracted from hippocampal cells by fluorometric method in the presence or absence of PHT. PHT inhibited cGDPR production in a concentration-dependent manner and IC$_{50}$ value was estimated as 12.74 ± 1.47 μM. It reduced cyclase activity in hippocampal cell lysate, but does not block it completely may be due to the presence of other ADPR cyclase enzymes in the cells that possibly are not inhibited completely by PHT or approximately equal binding affinity of CD38 to NAD$^+$ and PHT (interpreted from equal binding energy). According to previous reports, cyclic nucleotide was produced by CD38 is the main secondary messenger to release Ca^{2+} through ryanodine receptor/channels in ER membrane and also L-type calcium channel in cell membrane [11, 13, 14]. Therefore we measured NAD$^+$-induced Ca^{2+} influx as final results of CD38 function in the cells treated by different concentrations of PHT, results revealed significant inhibition of Ca^{2+} influx in hippocampus primary cells in a concentration dependent manner, half inhibition happened in 8.01 ± 1.02 μM. As previously reports, membrane depolarization via Na$^+$ current triggers Ca^{2+} entry to the cytosol, so it's possible all of the Na$^+$ blocking agents inhibits Ca^{2+} up-regulation [36]. Therefore we measured [Ca^{2+}]$_i$ in the presence of Na$^+$ specific blocker (TTX) that results showed Ca^{2+} influx induced by NAD$^+$ was not inhibited by TTX in the presence and absence of PHT. Our results confirmed PHT

reduces NAD$^+$ mediated Ca^{2+} influx through CD38 inhibition not sodium channel blocking.

A clear visualization of the cyclization process has been achieved and active site situation during substrate binding and catalysis described by detail that help us to understand how PHT inhibits CD38 cyclization activity (Fig. 1b). As molecular docking showed, PHT can bind to the active site and related lowest binding energy is −7.48 kcal/mol. Trp 125, Thp 186, Thr 221, Leu 145, Glu 226 and Ser 19 are main amino acids participate in substrate binding and catalytic activity of CD38 that interact with PHT rings according to Fig. 4 [25, 28]. As Fig. 3, PHT locates in deep of the active site cavity, close to the critical catalytic residue Glu 226 that inhibits NAD$^+$ interaction with catalytic groups. According to docking analysis NAD$^+$ binds to the CD38 active site with −7.76 kcal/mol binding energy, therefore CD38 binding affinity to the substrate and inhibitor is equal approximately. Close interaction of NAD$^+$ with the acidic residues of active site (Glu 226, Glu 260 and Asp 155) is difficult at cytosolic neutral pH when three acidic residues at the active site and nicotinic acid from substrate are negatively charged and electrostatically repulse each other [29]. But PHT is neutral molecule so could bind easily to the active site and interact with acidic residues rather than NAD$^+$. Totally according to hydrophobic nature of PHT hydrophobic and π interactions are important

in binding to the CD38 active site (Fig. 4d). Table 1 summarized kinetic parameters of cyclization activity calculated according to Michaelis-Menten and Lineweaver-Burk plots. Results showed inhibitor decreased affinity to the substrate by increasing apparent K_m. Although, catalytic activity reduced in the presence of PHT but enzyme reaches to V_{max} in high concentration of substrate. Results confirmed substrate competes with inhibitor and increased concentration of substrate neutralizes PHT presence in assay medium even in high does that refers to competitive type of inhibition.

Comparison of IC_{50} in cyclase activity and Ca^{2+} influx showed that half of the Ca^{2+} influx was inhibited by less concentration of PHT rather than cyclase activity possibly because: 1. cyclization and Ca^{2+} influx is two separate procedure and a lot of molecular events affected produced cADPR before Ca^{2+} release [37], or 2. PHT inhibited Ca^{2+} regulation through other pathways such as guanylyl cyclase and adenylyl cyclase suppression (cGMP and cAMP are other secondary messengers in Ca^{2+} regulation) as previously reported [8, 9]. Also presence of other Ca^{2+} entry pathways that does not affected by PHT such as N-Methyl-D-aspartic acid (NMDA) and α-amino-3-hydroxy-5-methyl-4-isoxazolepropionic acid (AMPA) receptors causes incompletely inhibition of Ca^{2+} influx [38].

Overall this study suggests CD38 pathway inhibition as a new mechanism to PHT biological activities as a drug. It could relief tonic clonic seizure, necrosis, neuropathic pain, inflammation, and heart arrhythmia that have common underlying pathophysiological mechanisms that are CD38 activation, membrane hyperexcitability and corresponding molecular changes. PHT inhibits sodium channel, guanylyl cyclase and CD38 so suppresses Ca^{2+} and Na^+ release and controls membrane depolarization and following cellular damages [30, 34, 39]. Therefore PHT could be used in the case of other pathological conditions are caused by activation of CD38/cADPR pathway such as oxidative stress, inflammation, sepsis-associated encephalopathy, allergic airway disease, ischemic brain injury and traumatic brain injury.

Compliance with ethical standards

References

1. Gallop K. Review article: phenytoin use and efficacy in the ED. Emerg Med Australas. 2010;22(2):108–18.
2. Jones GL, Wimbish GH, McIntosh WE. Phenytoin: basic and clinical pharmacology. Med Res Rev. 1983;3(4):383–434.
3. Guldiken B, Remi J, Noachtar H. Cardiovascular adverse effects of phenytoin. J Neurol. 2016;263(5):861–70.
4. Jensen TS. Anticonvulsants in neuropathic pain: rationale and clinical evidence. Eur J Pain. 2002;6:61–8.
5. Nelson M, Yang M, Dowle AA, Thomas JR, Brackenbury WJ. The sodium channel-blocking antiepileptic drug phenytoin inhibits breast tumour growth and metastasis. Mol Cancer. 2015;27(14):13.
6. Abdelsayed M, Sokolov S. Voltage gated sodium channels: pharmaceutical targets via anticonvulsants to treat epilepticsyndromes. Channels (Austin). 2013;7(3):146–52.
7. Backus KH, Pflimlin P, Trube G. Action of diazepam on the voltage-dependent Na+ current. Comparison with the effects of phenytoin, carbamazepine, lidocaine and flumazenil. Brain Res. 1991;548(1–2):41–9.
8. Ferrendelli JA, Kinscherf DA. Phenytoin: effects on calcium flux and cyclic nucleotides. Epilepsia. 1977;18(3):331–6.
9. Twombly DA, Yoshii M, Narahashi T. Mechanisms of calcium channel block by phenytoin. J Pharmacol Exp Ther. 1988;246(1):189–95.
10. Khaira A, Gupta A, Madhu SV, Khaira DD. Phenytoin induced severe disabling osteomalacia in a young male with seizure disorder. J Assoc Physicians India. 2008;56:376–8.
11. Bruzzone S, Moreschi I, Guida L, Usai C, Zocchi E, De Flora A. Extracellular NAD+ regulates intracellular calcium levels and induces activation of humangranulocytes. Biochem J. 2006;393(3):697–704.
12. Liu Q, Kriksunov IA, Graeff R, Munshi C, Lee HC, Hao Q. Structural basi for the mechanistic understanding of human CD38-controlled multiple catalysis. J Biol Chem. 2006;281(43):32861–9.
13. Partida-Sánchez S, Iribarren P, Moreno-García ME, Gao JL, Murphy PM, Oppenheimer N, et al. Chemotaxis and calcium responses of phagocytes to formyl peptide receptor ligands is differentially regulated by cyclic ADP ribose. J Immunol. 2004;172(3):1896–906.
14. Zündorf G, Reiser G. Calcium dysregulation and homeostasis of neural calcium in the molecular mechanisms of neurodegenerative diseases provide multiple targets for neuroprotection. Antioxid Redox Signal. 2011;14(7):1275–88.
15. Seibenhener ML, Wooten MW. Isolation and culture of hippocampal neurons from prenatal mice. J Vis Exp. 2012;65(3634):1–6.
16. Amina S, Hashii M, Ma WJ, Yokoyama S, Lopatina O, Liu HX, et al. Intracellular calcium elevation induced by extracellular application of cyclic-ADP-ribose or oxytocin is temperature-sensitive in rodent NG108-15 neuronal cells with or without exogenous expression of human oxytocin receptors. J Neuroendocrinol. 2010;22:460–6.
17. Brewer GJ. Serum-free B27/neurobasal medium supports differentiated growth of neurons from the striatum, substantia nigra, septum, cerebral cortex, cerebellum, and dentate gyrus. J Neurosci Res. 1995;42:674–83.
18. Hirst RA, Harrison C, Hirota K, Lambert DG. Measurement of [Ca²+]i in whole cell suspensions using fura-2. Methods Mol Biol. 2005;312:37–45.
19. Bagal SK, Marron BE, Owen RM, Storer RI, Swain NA. Voltage gated sodium channels as drug discovery targets. Channels (Austin). 2015;9(6):360–6.
20. Sun L, Adebanjo OA, Moonga BS, Corisdeo S, Anandatheerthavarada HK, Biswas G, et al. CD38/ADP-ribosyl cyclase: a new role in the regulation of osteoclastic bone resorption. J Cell Biol. 1999;146(5):1161–72.
21. Morris GM, Huey R, Lindstrom W, Sanner MF, Belew RK, Goodsell DS, et al. AutoDock4 and AutoDockTools4: automated docking with selective receptor flexibility. J Comput Chem. 2009;30:2785–91.
22. Rizvi SMD, Shakil S. Haneef M. a simple click by click protocol to perform docking: AutoDock 4.2 made easy for non-bioinformaticians. EXCLI J. 2013;12:831–57.
23. Graeff RM, Mehta K, Lee HC. GDP-ribosyl cyclase activity as a measure of CD38 induction by retinoic acid in HL-60 cells. Biochem Biophys Res Commun. 1994;205(1):722–7.

24. Liu Q, Graeff R, Kriksunov IA, Jiang H, Zhang B, Oppenheimer N, et al. Structural basis for enzymatic evolution from a dedicated ADP-ribosyl cyclase to a multifunctional NAD hydrolase. J Biol Chem. 2009;284:27637–45.

25. Liu Q, Kriksunov IA, Graeff R, Munshi C, Lee HC, Hao Q. Structural basis for the mechanistic understanding of human CD38-controlled multiple catalysis. J Biol Chem. 2006;281:32861–9.

26. Meyer EA, Castellano RK, Diederich F. Interactions with aromatic rings in chemical and biological recognition. Angew Chem Int Ed Engl. 2003;42(11):1210–50.

27. Lucas X, Bauzá A, Frontera A, Quiñonero D. A thorough anion-π interaction study in biomolecules: on the importance of cooperativity effects. Chem Sci. 2016;7(2):1038–50.

28. Zhang H, Graeff R, Lee HC, Hao Q. Crystal structures of human CD38 in complex with NAADP and ADPRP. Messenger. 2013;2(1):44–53.

29. Graeff R, Liu Q, Kriksunov IA, Hao Q, Lee HC. Acidic residues at the active sites of CD38 and ADP-ribosyl cyclase determine nicotinic acid adenine dinucleotide phosphate (NAADP) synthesis and hydrolysis activities. J Biol Chem. 2006;281(39):28951–7.

30. Peng QY, Wang YM, Chen CX, Zou Y, Zhang LN, Deng SY, et al. Inhibiting the CD38/cADPR pathway protected rats against sepsis associated brain injury. Brain Res. 2018;1678:56–63.

31. Antonelli A, Ferrannini E. CD38 autoimmunity: recent advances and relevance to human diabetes. J Endocrinol Investig. 2004;27(7):695–707.

32. Thornton PD, Fernandez C, Giustolisi GM, Morilla R, Atkinson S, A'Hern RP, et al. CD38 expression as a prognostic indicator in chronic lymphocytic leukaemia. Hemato J. 2004;5:145–51.

33. Roussanov BV, Taylor JM, Giorgi JV. Calculation and use of an HIV-1 disease progression score. AIDS. 2000;14(17):2715–22.

34. Gul R, Park JH, Kim SY, Jang KY, Chae JK, Ko JK, et al. Inhibition of ADP-ribosyl cyclase attenuates angiotensin II induced cardiac hypertrophy. Cardiovasc Res. 2009;81(3):582–91.

35. Moreau C, Liu Q, Graeff R, Wagner GK, Thomas MP, Swarbrick JM, et al. CD38 Structure-Based Inhibitor Design Using the N1-Cyclic Inosine 59-Diphosphate Ribose Template. PLoS One. 2013;8(6):66247.

36. Bose T, Cieślar-Pobuda A, Wiechec E. Role of ion channels in regulating Ca^{2+} homeostasis during the interplay between immune and cancer cells. Cell Death Dis. 2015;6:e1648.

37. Wei W, Graeff R, Yue J. Roles and mechanisms of the CD38/cyclic adenosine diphosphate ribose/Ca^{2+} signaling pathway. World J Biol Chem. 2014;5(1):58–67.

38. Lee KH, Park JY, Kim K. NMDA receptor-mediated calcium influx plays an essential role in myoblast fusion. Volume 578, Issues 1–2, 3 December 2004, Pages 47–52.

39. Zhang Y, Chen X, Gueydan C, Han J. Plasma membrane changes during programmed cell deaths. Cell Res. 2018;28(1):9–21.